1-2011

Biochemical Characterization of Bacteriophage T4 Mre11-Rad50 Complex

Timothy J. Herdendorf
Iowa State University

Dustin William Albrecht
Iowa State University, dustinalbrecht@gmail.com

Stephen J. Benkovic
Pennsylvania State University - Main Campus

Scott W, Nelson
Iowa State University, swn@iastate.edu

Biochemical Characterization of Bacteriophage T4 Mre11-Rad50 Complex

Abstract

The Mre11-Rad50 complex (MR) from bacteriophage T4 (gp46/47) is involved in the processing of DNA double-strand breaks. Here, we describe the activities of the T4 MR complex and its modulation by proteins involved in homologous recombination. T4 Mre11 is a Rad50- and Mn^{2+}-dependent dsDNA exonuclease and ssDNA endonuclease. ATP hydrolysis is required for the removal of multiple nucleotides via dsDNA exonuclease activity but not for the removal of the first nucleotide or for ssDNA endonuclease activity, indicating ATP hydrolysis is only required for repetitive nucleotide removal. By itself, Rad50 is a relatively inefficient ATPase, but the presence of Mre11 and dsDNA increases ATP hydrolysis by 20-fold. The ATP hydrolysis reaction exhibits positive cooperativity with Hill coefficients ranging from 1.4 for Rad50 alone to 2.4 for the Rad50-Mre11-DNA complex. Kinetic assays suggest that approximately four nucleotides are removed per ATP hydrolyzed. Directionality assays indicate that the prevailing activity is a 3′ to 5′ dsDNA exonuclease, which is incompatible with the proposed role of MR in the production of 3′ ssDNA ends. Interestingly, we found that in the presence of a recombination mediator protein (UvsY) and ssDNA-binding protein (gp32), Mre11 is capable of using Mg^{2+} as a cofactor for its nuclease activity. Additionally, the Mg^{2+}-dependent nuclease activity, activated by UvsY and gp32, results in the formation of endonuclease reaction products. These results suggest that gp32 and UvsY may alter divalent cation preference and facilitate the formation of a 3′ ssDNA overhang, which is a necessary intermediate for recombination-mediated double-strand break repair.

Keywords

DNA-binding Protein, DNA Damage, DNA Enzymes, DNA Recombination, DNA Repair, DNA Exonuclease, Gene Product 46, gp46, Gene Product 47, gp47

Disciplines

Biochemistry, Biophysics, and Structural Biology | Chemistry | Molecular Biology

Comments

This article is from *Journal of Biological Chemistry* 286 (2011): 2382, doi: 10.1074/jbc.M110.178871. Posted with permission.

THE JOURNAL OF BIOLOGICAL CHEMISTRY VOL. 286, NO. 4, pp. 2382–2392, January 28, 2011

Biochemical Characterization of Bacteriophage T4 Mre11-Rad50 Complex*

Received for publication, August 30, 2010, and in revised form, November 2, 2010 Published, JBC Papers in Press, November 15, 2010, DOI 10.1074/jbc.M110.178871

Timothy J. Herdendorf[‡], Dustin W. Albrecht[‡], Stephen J. Benkovic[§1], and Scott W. Nelson[‡2]

From the [‡]Department of Biochemistry, Biophysics, and Molecular Biology, Iowa State University, Ames, Iowa 50011 and the [§]Department of Chemistry, 414 Wartik Laboratory, The Pennsylvania State University, University Park, Pennsylvania 16802

The Mre11-Rad50 complex (MR) from bacteriophage T4 (gp46/47) is involved in the processing of DNA double-strand breaks. Here, we describe the activities of the T4 MR complex and its modulation by proteins involved in homologous recombination. T4 Mre11 is a Rad50- and Mn^{2+}-dependent dsDNA exonuclease and ssDNA endonuclease. ATP hydrolysis is required for the removal of multiple nucleotides via dsDNA exonuclease activity but not for the removal of the first nucleotide or for ssDNA endonuclease activity, indicating ATP hydrolysis is only required for repetitive nucleotide removal. By itself, Rad50 is a relatively inefficient ATPase, but the presence of Mre11 and dsDNA increases ATP hydrolysis by 20-fold. The ATP hydrolysis reaction exhibits positive cooperativity with Hill coefficients ranging from 1.4 for Rad50 alone to 2.4 for the Rad50-Mre11-DNA complex. Kinetic assays suggest that approximately four nucleotides are removed per ATP hydrolyzed. Directionality assays indicate that the prevailing activity is a 3′ to 5′ dsDNA exonuclease, which is incompatible with the proposed role of MR in the production of 3′ ssDNA ends. Interestingly, we found that in the presence of a recombination mediator protein (UvsY) and ssDNA-binding protein (gp32), Mre11 is capable of using Mg^{2+} as a cofactor for its nuclease activity. Additionally, the Mg^{2+}-dependent nuclease activity, activated by UvsY and gp32, results in the formation of endonuclease reaction products. These results suggest that gp32 and UvsY may alter divalent cation preference and facilitate the formation of a 3′ ssDNA overhang, which is a necessary intermediate for recombination-mediated double-strand break repair.

Replication in T4[3] phage is initiated through origin-dependent and -independent pathways (1). The origin-dependent pathway relies on the host cell RNA polymerase to synthesize an mRNA transcript, which is then processed and remains stably bound at the origin in what is known as an R-loop (2). The origin-independent pathway relies on homologous recombination (HR) within or between phage genome(s) (3). HR is essential to the lifecycle of T4 phage because the origin-dependent mode of initiation ends after only a few rounds of replication (4). A strong link between recombination and DNA repair was recognized early on using T4 phage as a model system (for review, see Ref. 5). In the late 1960s it was reported that certain genes when mutated severely affected replication, recombination, and DNA repair (6). Indeed, the current models of DNA double-strand break (DSB) repair share many of the same steps as recombination-mediated initiation of replication (7, 8).

DSBs are one of the most lethal forms of DNA damage, and unless repaired they may lead to gross chromosomal rearrangements, deletions, duplications, or cell death (9, 10). DSBs are caused by exogenous agents such as ionizing and ultraviolet radiation and chemical mutagens or endogenous agents such as reactive oxygen species. In eukaryotic cells, DSBs are repaired through two pathways, non-homologous end joining (NHEJ) and HR; however, in T4 phage it appears that all DSBs are repaired through HR (4, 11).

The biochemical activities necessary for HR have been identified, and in most cases, the proteins responsible for these activities are known (8, 12, 13). HR begins with the processing of a dsDNA end to produce a 3′ ssDNA overhang. In *Escherichia coli*, this step is performed by the well characterized helicase-nuclease complex, RecBCD (14). However, the genomes of eukaryotes, Archaea, and T4 phage do not contain any obvious RecBCD orthologs, and it appears that the Mre11-Rad50 (MR) complex together with other proteins specific to each system perform the analogous function (15). After end resection, the recombinase (RecA or RecA ortholog) binds to the ssDNA and forms a nucleoprotein filament that is capable of undergoing strand invasion and exchange with homologous DNA templates (16). This strand invasion event produces a D-loop structure that acts as a scaffold and primer for DNA synthesis (17). The HR pathway ends with either the resolution of the Holliday junction by a nuclease or the dissociation and strand annealing of the newly synthesized DNA strands (18).

In T4 phage, all of the proteins implicated in HR are well characterized except for Mre11 and Rad50 (gp47 and gp46, respectively) (19–24). In eukaryotic systems, the MR complex has long been associated with the repair of DSBs (25). In *Saccharomyces cerevisiae*, null mutants of Mre11, Rad50, or Xrs2

* This work was supported, in whole or in part, by National Institutes of Health Grant GM013306 (to S. J. B.). This work was also supported by Carver Trust Young Investigator Grant 10-3603 (to S. W. N.) and by Iowa State University institutional support (to S. W. N.).

[1] To whom all correspondence may be addressed. Tel.: 814-865-2882; Fax: 814-865-2973; E-mail: sjb1@psu.edu.

[2] To whom all correspondence may be addressed. Tel.: 515-294-3434; Fax: 515-294-0453; E-mail: swn@iastate.edu.

[3] The abbreviations used are: T4 phage, bacteriophage T4; DSB, double-strand break; HR, homologous recombination; gp46, T4 gene product 46; gp47, T4 gene product 47; gp32, T4 gene product 32; UvsY, UV sensitivity protein Y; MR, Mre11-Rad50; SMC, structural maintenance of chromosomes; ABC, ATP binding cassette; 2-AP, 2-aminopurine; RDR, recombination-dependent DNA replication; PEI, polyethyleneimine; AMP-PNP, adenosine 5′-(β,γ-imino)triphosphate.

(a third protein found in the *S. cerevisiae* MR complex) are unable to initiate and process meiotic DSBs and are sensitive to DNA-damaging agents that produce DSBs such as ionizing radiation or methylmethane sulfonate (18). This led to a proposal that the MR complex is responsible for resection (5′ to 3′ dsDNA exonuclease activity) of DSBs (26). However, *in vitro*, the eukaryotic MR complex exhibits a 3′ to 5′ dsDNA exonuclease and ssDNA endonuclease activity (27, 28). The products of these activities are not 3′ ssDNA overhangs, and therefore, the true function of the MR complex has been elusive.

Rad50 is a member of the SMC (structural maintenance of chromosome family of proteins), which are in turn members of the ATP binding cassette (ABC) superfamily. All known ABC protein family members are dimeric and bind ATP at the interface between two monomers. It is thought that the energy of ATP hydrolysis is used to drive conformational changes within the ABC protein/domain, which are then propagated to other associated proteins or domains (29). Most ABC protein family members are membrane transporters, such as the Cystic Fibrosis Transmembrane Regulator transporter and *p*-glycoprotein, which, when mutated, cause cystic fibrosis and multidrug resistance, respectively (30). In addition to transporters, the DNA repair enzymes MutS and RecF are ABC proteins. The structure of the nucleotide binding domain of *Pyrococcus furiosus* (*Pfu*) Rad50 has been solved in the apo- and ATP-bound forms (31). The structures reveal significant conformational rearrangements that occur upon ATP binding and/or hydrolysis, which are thought to control the activity of Mre11 (32). Rad50 and related SMC proteins have an unusual architecture where the ABC protein motifs are split by a long coiled-coil region. In Rad50, the apex of the coiled-coil contains a conserved C*XX*C motif, which dimerizes with a second Rad50 monomer to create a zinc binding site similar to a zinc finger (33). The purpose of the coiled-coil motif is not entirely clear, but it is thought to be involved in tethering the DSB to a homologous template or tethering the two ends of the DSB to each other (15). In eukaryotes the coiled-coil domain contains ~900 amino acids, whereas in T4 phage the coiled-coil contains around 200 residues. Presumably, the long coiled-coil region in eukaryotes is responsible for the expression difficulties encountered with the eukaryotic proteins. To date, only microgram quantities of eukaryotic Rad50 have been purified (27, 28, 34, 35).

Mre11 is a member of the Ser/Thr protein phosphatase family, which contains four conserved motifs and requires divalent cations for activity (36). Although the mutation of Mre11 has only a mild effect in *S. cerevisiae* (37), in human cells the nuclease activity of Mre11 is essential, and its inactivation results in embryonic lethality and extreme sensitivity to ionizing radiation (38). In humans, inherited Mre11 mutations cause ataxia telangiectasia-like disorder, the symptoms of which include hypersensitivity to ionizing radiation and cerebellar degeneration (39). The *Pfu* Mre11 protein is dimeric and binds dsDNA near the dimeric interface (40). As mentioned above, *in vitro* assays reveal that Mre11 possesses a 3′ to 5′ dsDNA exonuclease activity along with ssDNA endonuclease activity (27).

Recently, several papers have clarified the role of the MR complex in the processing of DSBs. The Mimitou and Symington (41) and Ira and co-workers (42) laboratories simultaneously demonstrated that DSBs are processed through a two-step mechanism involving the MR complex, Sae2, ExoI, Sgs1, and Dna2. In the initial step, the MRX complex, in conjunction with Sae2, removes ~100–200 bases from the 5′ end of the DNA. In the second step, ExoI or Sgs1 with Dna2 catalyze rapid and processive removal of thousands of bases from the 5′ end of the DNA. The resulting 3′ ssDNA overhang can undergo Rad51-dependent HR or Rad52-dependent single-strand annealing.

In this report, we express, purify, and biochemically characterize the MR DNA repair complex from T4 phage. We find that the T4 MR complex shares all the same activities as its eukaryotic counterparts, but expression and purification of the Rad50 and Mre11 proteins is rapid and yields milligram quantities of purified proteins, which allows for the mechanistic examination of the complex. Our experiments indicate that the T4 MR complex is a DNA-activated ATPase, a Mn^{2+}-dependent ssDNA endonuclease. and a Mn^{2+}- and ATP-dependent 3′ to 5′ dsDNA exonuclease. ATP hydrolysis is positively cooperative with respect to ATP concentration, and during the exonuclease reaction four nucleotides are removed per ATP hydrolyzed. Although the observed 3′ to 5′ dsDNA exonuclease activity is incompatible with its proposed *in vivo* function, we find that the presence of two T4 recombination proteins, UvsY and gp32, alter the nuclease activity of the MR complex, which may promote the formation of a 3′ ssDNA recombinogenic end.

EXPERIMENTAL PROCEDURES

Cloning, Expression, and Purification of T4 Mre11 and wt-Rad50 and K42M-Rad50—The open reading frames for gp46 and 47 were PCR-amplified from bacteriophage T4 genomic DNA (Sigma) and cloned into the pTYB1 expression vector (New England Biolabs) using the NdeI and SapI restriction sites using the following primers: T4Rad50-NdeF, 5′-GGTGGTCATATGAAGAATTTTAAACTTAATAG; T4Rad50-SapR, 5′-GGTGGTTGCTCTTCCGCATTAAACCATTACAGTAAATCG; T4Mre11-NdeF, 5′-GGTGGTCATATGAAAATTTTAAATTTAGGTG; T4Mre11-SapR, 5′-GGTGGTTGCTCTTCCGCATCATTGTGTTGCCTCTACATATAG. The K42M-Rad50 mutant was generated using the QuikChange™ protocol (Stratagene) using the mutagenic forward primer, K42M-Rad50F (5′-GGACGAAATGGCGGTGGTA**TG**TCTACTATGCTAGAAGCC-3′, where the mutant codon is highlighted in bold). The reverse mutagenic primer is the reverse complement of the forward. The pTYB1 vector creates a fusion between the gene of interest and a self-cleavable intein/chitin binding domain purification tag. The gp46-pTYB1, K42M-gp46-pTYB1, and gp47-pTYB1 expression vectors were separately transformed into BL21(DE3) cells and plated on LB-agar plates containing 150 μg/ml ampicillin. A single colony from each plate was used to separately inoculate 50-ml flasks of LB-ampicillin that were shaken for 16 h at 37 °C. 10 ml of starter culture was used to inoculate four 1-liter flasks of LB-ampicillin per protein, which were shaken at 225 rpm at

37 °C to an A_{600} of 0.8. The flasks were then cooled to 18 °C, and expression was induced by the addition of 0.2 mM isopropyl 1-thio-β-D-galactopyranoside. After 16 h the cells were collected by centrifugation at 8000 × *g* for 8 min, and pellets were frozen at −20 °C.

The purification scheme for T4 Rad50 (including K42M-Rad50) and Mre11 was identical through the chitin column elution step. A frozen cell pellet (~15 g) was resuspended in 75 ml of ice-cold lysis buffer (20 mM Tris-HCl, 500 mM NaCl, 1 mM EDTA, pH 8.0) and lysed by sonication. All purification steps were carried out at 4 °C. The lysed cells were then centrifuged at 18,000 × *g* for 60 min. The cell-free extract was loaded onto a column packed with 5 ml of chitin beads (New England Biolabs). The column was then washed with 100 ml of lysis buffer followed by an overnight wash with 1.5 liters of wash buffer (20 mM Tris-HCl, 1 M NaCl, 1 mM EDTA, pH 8.0). Cleavage of the intein-chitin binding domain tag was initiated by washing the column with 3 column volumes of cleavage buffer (20 mM Tris-HCl, 200 mM NaCl, 1 mM EDTA, 75 mM β-mercaptoethanol, pH 8.0) before stopping the buffer flow. The chitin column was incubated in cleavage buffer for 16 h at 4 °C followed by elution of the tag-less protein. Mre11 was dialyzed twice against 1 liter of storage buffer (20 mM Tris-HCl, 200 mM NaCl, 20% glycerol, pH 8.0), concentrated to 50–100 μM, dispensed into small aliquots, and frozen at −80 °C. Rad50 was loaded directly onto a 20-ml cellulose phosphate (P11, Whatman) column followed by a 10-column volume wash with P11 wash buffer (20 mM Tris-HCl, 200 mM NaCl, pH 8.0). T4 Rad50 was eluted from the P11 column with P11 elution buffer (20 mM Tris-HCl, 400 mM NaCl, 20% glycerol, pH 8.0), concentrated to 25–50 μM, dispensed into aliquots, and frozen at −80 °C. The extinction coefficients for determining the concentration of T4 Mre11 and Rad50 are 69,130 and 33,140 $cm^{-1}\ M^{-1}$, respectively.

DNA Substrates—The M13 phage ssDNA was purified using PEG precipitation and phenol/chloroform extraction (43). The 50-bp dsDNA substrate was prepared by annealing equal amounts of two complementary oligonucleotides with the following sequences: ds50-mer_top (5′-CTC TTG GTG ATT ATG ATG GTT GCA ATA CAT TTA ATT TCA TTA TCA ATT AG-3′) and ds50-mer_bottom (5′-CTA ATT GAT AAT GAA ATT AAA TGT ATT GCA ACC ATC ATA ATC ACC AAG AG-3′). The 17 position 2-aminopurine (2-AP)-containing substrate was of identical sequence to ds50-mer_top except that the adenine at position 17 (relative to the 3′ end of the DNA) was replaced with 2-AP. The DNA substrate with the 2-AP at the 1 position (3′ end) had an identical sequence to ds50-mer_top except that the 3′ G was replaced with 2-AP. To prepare the 5′-labeled 50-bp DNA, the annealed duplex was diluted to a concentration of 5 μM and treated with polynucleotide kinase (New England Biolabs) and 10 μCi of [γ-^{32}P]ATP in a volume of 20 μl (total ATP concentration of 0.165 μM) for 30 min. After 30 min cold ATP was added to a final concentration of 100 μM and allowed to react for 30 additional minutes. The reaction was then quenched at 65 °C for 20 min followed by removal of free nucleotides by passing the reaction through a G-25 Sephadex spin column. To prepare the 3′-labeled 50-bp DNA, the annealed duplex was diluted to a concentration of 10 μM and treated with 5 units of T4 DNA polymerase (Promega) in the presence of 1 mM dCTP, dTTP, and dATP in a final volume of 20 μl for 5 min. The reaction was then heated at 65 °C for 20 min to inactivate the T4 polymerase. After heat inactivation, 5 units of T4 exonuclease-deficient polymerase was added to the reaction along with 20 μCi of [α-^{32}P]dGTP in a final volume of 38 μl. The reaction was allowed to proceed at 37 °C for 30 min before the addition of 2 μl of 0.1 mM dGTP. The reaction was continued for 30 additional minutes, then heat-inactivated for 20 min at 65 °C. Finally, the reaction was passed through a G-25 Sephadex spin column to remove free nucleotides and precipitated protein. The uniformly labeled 1.68-kb dsDNA was prepared by performing a 100-μl PCR reaction in Taq polymerase buffer (Promega) using 5 units of Taq polymerase, 40 μCi of [α-^{32}P]dGTP, 0.1 mM cold dNTP mix, 1 μM gp46-Nde-F, 1 μM gp46-Sap-R, and 100 ng of the gp46-pTYB1 vector. The labeled PCR product was purified using the Qiagen PCR purification kit following the manufacturer's protocol and quantitated using liquid scintillation counting.

Nuclease and ATP Hydrolysis Assays—The standard conditions for the nuclease reactions were 20 mM Tris-HCl, 50 mM KCl, 2 mM ATP, pH 7.6, and a divalent metal concentration indicated in the figure legends. The concentrations of ssDNA, dsDNA, Rad50, and Mre11 varied for each experiment and are given in the individual figure legends. The gp32 and UvsY proteins were purified by intein/chitin-based affinity chromatography as described (44). Reactions that were analyzed using 1% Tris acetate-EDTA-agarose gels (Fig. 1) were quenched in 5 mM Tris-HCl, pH 7.5, 200 mM EDTA, 0.2% orange G, 0.015% bromphenol blue, 0.015% xylene cyanol FF, and 7.5% Ficoll 400. The agarose gels were stained with 10 μg/ml ethidium bromide for 30 min before visualization. Reactions that were analyzed using Tris borate-EDTA-urea-PAGE (15% polyacrylamide) (Figs. 2 and 7) were quenched with 50 mM EDTA, 95% formamide, 0.015% xylene cyanol FF, and 0.015% bromphenol blue. The PAGE gels ran for 2 h at 35 mA followed by overnight exposure to a PhosphorImager plate and subsequent analysis using a Storm PhosphorImager and ImageQuant software (GE Healthcare). The reactions that were analyzed using PEI-TLC (Figs. 4, *C* and *D*, 5*A*, and 6) were quenched in an equal volume of 200 mM EDTA. The quenched samples were then spotted onto the PEI plates (1–2 μl volume) and developed in 300 mM KP_i, pH 7.0. The TLC plate was then dried and exposed for 2 h to the PhosphorImager plate followed by analysis using the Storm PhosphorImager and ImageQuant software.

To examine the steady-state exonuclease activity of the MR complex, we employed a real-time continuous assay based on the enhancement of fluorescence when the nucleotide analog, 2-AP, is excised from DNA (45). The assay was carried out at 30 °C using excitation and emission wavelengths of 310 and 375 nm, respectively, on a Cary Eclipse (Varian) spectrofluorometer. The reaction buffer contained 50 mM Tris-HCl, pH 7.6, 50 mM KCl, 5 mM $MgCl_2$, 0.3 mM $MnCl_2$, 0.1 μM MR complex, and 1.3 μM 2-AP labeled dsDNA. The reactions were monitored for ~5–10 min, and velocities were determined using at least three min of the time course.

To determine the steady-state ATP hydrolysis activity of Rad50 and the MR complex, we employed the standard coupled fluorometric ATP hydrolysis assay (46) carried out at 30 °C using excitation and emission wavelengths of 340 and 460 nm, respectively, on either a SLM-Aminco (SLM Instruments, Inc.) or a Cary Eclipse spectrofluorometer (Varian). The reaction buffer contained 50 mM Tris-HCl, pH 7.6, 50 mM KCl, 5 mM $MgCl_2$, 50 μM NADH, 150 μM phosphoenolpyruvate, 6.67 units/ml pyruvate kinase, and 10 units/ml lactate dehydrogenase. In reactions where Mre11 was included, its concentration was always in slight excess over the Rad50 concentration. In reactions containing DNA, its concentration was held in excess over that of Rad50 or the MR complex and well above the $K_{activation}$ for DNA.[4] Steady-state rate constants were determined using Sigmaplot 10.0/Enzyme Kinetics Module 1.3 (Systat Software, Inc.).

RESULTS

Expression and Purification of T4 Rad50 and Mre11—Overexpression of eukaryotic Mre11 and Rad50 requires the use of either *S. cerevisiae* or insect cells and yields only microgram amounts of purified protein (27, 28, 34). Moreover, eukaryotic Rad50 is difficult to overexpress separately and requires co-expression of Mre11 to form significant amounts of soluble protein (47). We have achieved overexpression and purification of T4 Rad50 by constructing a C-terminal fusion with the intein/chitin binding domain provided by the pTYB1 vector. The chitin binding domain facilitates capture by chitin beads, and the intein domain allows for reductant-mediated self- cleavage (48). After self-cleavage, the Rad50 protein that elutes from the chitin beads contains a strong absorbance at 260 nm, indicating the presence of bound nucleotides or nucleic acids. Dialysis of the protein did not reduce 260-nm absorbance; therefore, we applied the eluted protein to phosphocellulose resin. The material that strongly absorbed at 260 nm was not retained by the column, but nearly 100% of the protein was efficiently bound. After a buffer wash, the NaCl concentration was increased from 200 to 400 mM, which eluted the Rad50 protein. This protein had a 280/260 nm ratio of 1.98, indicating that there is little to no nucleotide or nucleic acid contamination in our preparation of Rad50. Additionally, no appreciable enhancement of DAPI dye fluorescence was observed upon the addition of protease-K-digested Rad50, indicating the absence of contaminating DNA (data not shown). The overall yield for T4 Rad50 was ~3 mg of protein per liter of LB (Fig. 1*A*, *third lane*). The Rad50 Walker A motif mutant, K42M-Rad50, behaved essentially identical to the wild-type protein.

T4 Mre11 was also C-terminal-fused to the intein/chitin binding domain provided by the pTYB1 vector. Mre11 was expressed in an identical fashion as Rad50 but was ~10-fold more abundant in the cell-free extracts as compared with Rad50. Additionally, the 280/260-nm absorbance ratio indicated that no nucleotides or nucleic acids were present in the protein that eluted from the chitin column. Therefore, only a single column was necessary to achieve the desired level of purity. The overall yield for T4 Mre11 was ~25 mg of protein/liter of LB (Fig. 1*A*, *second lane*).

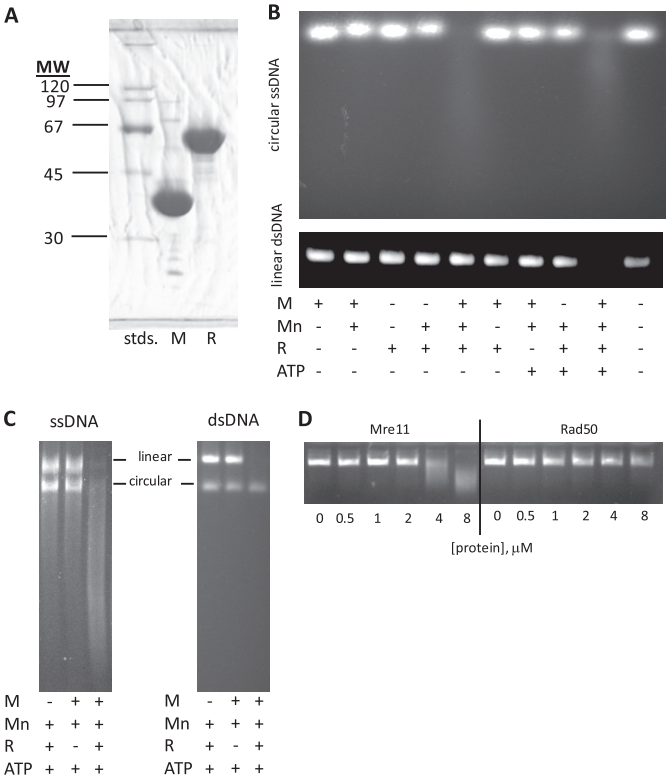

FIGURE 1. *A*, SDS-PAGE analysis of purified bacteriophage T4 Mre11 and Rad50 is shown. Approximately 20 μg of protein was separated using 12% SDS-PAGE and stained with Coomassie Blue R-250. The *first through third lanes* are molecular weight markers (*stds.*), Mre11 (*M*), and Rad50 (*R*), respectively. *B*, the requirement for nuclease activity using circular ssDNA (0.4 μg) and linear dsDNA (0.4 μg) as substrates is shown. The concentrations of $MnCl_2$ (*Mn*), Mre11 (*M*), Rad50 (*R*), and ATP were 5 mM, 0.3 μM, 0.3 μM, and 2 mM, respectively. The reaction was performed at 37 °C for 30 min. The products of the reaction were analyzed using Tris acetate-EDTA-agarose gel electrophoresis and stained with ethidium bromide. *C*, nuclease reactions using circular and linearized forms of ss and dsDNA (0.4 μg each) using $MnCl_2$, Rad50 (*R*), Mre11 (*M*), and ATP concentrations of 5 mM, 0.3 μM, 0.3 μM, and 2 mM, respectively, are shown. *D*, nuclease assay carried out for 60 min using dsDNA (0.4 μg), 5 mM $MnCl_2$, 2 mM ATP, and the indicated concentrations of either Mre11 or Rad50 are shown.

Requirements for Mre11 Nuclease Activity—To determine the requirements for the predicted Mre11 nuclease activity, we performed agarose gel electrophoresis-based nuclease assays. The metal, protein, and ATP dependence was tested using circular ssDNA (M13mp18) and linear dsDNA (Fig. 1*B*). The ssDNA nuclease reaction required the presence of Mre11, $MnCl_2$, and Rad50. Under these conditions, replacement of $MnCl_2$ with $MgCl_2$ or $ZnCl_2$ resulted in no observable nuclease activity (data not shown). The dsDNA nuclease reaction required the same components; however, ATP was also necessary for nucleolytic degradation of the dsDNA. In addition to defining the components required for nuclease activity, these results strongly argue against the presence of a contaminating nuclease in our preparations of either Mre11 or Rad50 (as both proteins are required). We next tested the endo/exo activity using linear and circular ssDNA or dsDNA (Fig. 1*C*). These reactions indicate that the T4 MR complex contains ssDNA endonuclease activity (*i.e.* both linear and circular ssDNA are degraded) and dsDNA exonuclease activ-

[4] T. J. Herdendorf and S. W. Nelson, unpublished data.

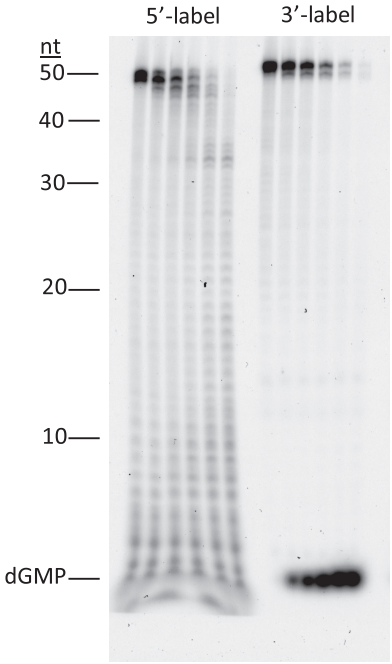

FIGURE 2. **Polarity of T4 Mre11-Rad50 dsDNA exonuclease activity.** Analysis of nuclease reaction products using 16% UREA-PAGE is shown. The reaction was carried out at 37 °C, and the time points for each lane are 0, 0.5, 1, 2, 4, and 8 min. The concentrations of dsDNA, Mre11, Rad50, $MnCl_2$, and ATP were 0.5 μM, 0.1 μM, 0.1 μM, 5 mM, and 2 mM, respectively. The dGMP band was identified by comparison to a reaction analyzed using PEI-TLC. *nt*, nucleotides.

ity (*i.e.* only linear dsDNA is degraded). We also confirmed that the nuclease activity resides in the Mre11 subunit (Fig. 1*D*). This assignment is predicted based on sequence analysis; however, the nuclease subunit of the T4 MR complex had been previously assigned to Rad50 rather than Mre11 (49). We separately assayed the ability of Mre11 and Rad50 to degrade dsDNA at elevated concentrations of protein in the presence of $MnCl_2$ and ATP (Fig. 1*D*). Although the activity is >100-fold less than the MR complex, as expected, the nuclease activity resides within the Mre11 subunit.

Polarity of the dsDNA Exonuclease Activity of the MR Complex—To determine the nuclease polarity of the MR complex, we compared the product pattern resulting from nuclease activity using either 5′- or 3′-labeled 50-bp dsDNA (Fig. 2). The presence of intermediate-length products in reactions using the 5′-labeled DNA substrate and their absence in reactions with the 3′-labeled DNA substrate is consistent with a 3′ to 5′ exonuclease.

Steady-state ATP Hydrolysis Activity of Rad50 and the MR Complex—Rad50 is part of the ABC protein superfamily, and it is known that Rad50 catalyzes the hydrolysis of ATP (50). Additionally, the data shown in Fig. 1 indicate that ATP is necessary for the dsDNA exonuclease activity of the MR complex. For these reasons we examined the Mg-ATP hydrolysis activity of the MR under conditions where the nuclease activity is negligible (*i.e.* in the absence of Mn^{2+}). We determined the steady-state Mg-ATP hydrolysis rate constants for Rad50 and the MR complex with and without DNA (Table 1). Because these reactions are performed without Mn^{2+}, DNA is not consumed and can be considered an activator rather than

TABLE 1
Steady-state kinetic constants for bacteriophage T4 Rad50 ATP hydrolysis

Protein	k_{cat}	K_m	Hill
	s^{-1}	μM	*n*
Rad50[a]	0.146 ± 0.003	16.0 ± 0.8	1.4 ± 0.1
Rad50/DNA[b]	0.100 ± 0.003	54.1 ± 0.6	1.2 ± 0.1
Mre11/Rad50[c]	0.226 ± 0.006	41.5 ± 0.3	1.5 ± 0.1
Mre11/Rad50/DNA[d]	3.2 ± 0.1	49.2 ± 1.6	2.4 ± 0.2

[a] Concentrations were 0.5 μM Rad50.
[b] Concentrations were 0.5 μM Rad50 and 2 μM DNA.
[c] Concentrations were 0.5 μM Rad50 and 0.63 μM Mre11.
[d] Concentrations were 0.08 and 0.3 μM Rad50, 0.13 and 0.5 μM Mre11, and 0.33 and 1 μM DNA.

a substrate. We found that by itself, Rad50 is a relatively weak ATPase, and the rate of ATP hydrolysis is sigmoidally dependent on the concentration of ATP. The data fit best to the Hill equation,

$$v = \frac{V_{max} \cdot [S^n]}{K_m{}^n + [S]^n} \quad \text{(Eq. 1)}$$

where v is velocity, V_{max} is the maximal velocity at saturating substrate concentration, K_m is the Michaelis constant (substrate concentration where $v = 0.5 \cdot V_{max}$), and n is the Hill coefficient. An F test was employed to justify the use of the Hill equation over the standard Michaelis-Menten equation. The data fitting yielded a k_{cat} of 0.15 s^{-1}, a K_m of 16 μM, and a Hill coefficient of 1.4. The addition of Mre11 results in minor changes in the kinetic constants with 1.5- and 2.6-fold increases in the k_{cat} (0.226 s^{-1}) and K_m (41.5 μM), respectively, and no significant change in the Hill coefficient (1.5). The addition of dsDNA to Rad50 alone caused a 3.4-fold increase in K_m (54 μM) and very minor decreases in k_{cat} (0.10 s^{-1}) and the Hill coefficient (1.2). The addition of DNA to the MR complex caused a 14-fold increase in the k_{cat} relative to the MR complex alone (3.2 s^{-1}), an increase in Hill coefficient (2.4), and no significant change in the K_m (49.2 μM). The large activation of ATPase activity is specific to linear dsDNA as circular plasmid DNA or a 50-base ssDNA oligonucleotide had no effect (data not shown). Mutation of the predicted Walker A lysine to methionine (K42M-Rad50) reduced the observed ATPase activity ~200-fold compared with Rad50 alone and ~4000-fold compared with the MR-DNA complex. This large decrease in activity is expected given the role the Walker A lysine plays in stabilizing negative charge that forms during the transition state for ATP hydrolysis. The residual activity that is observed represents the upper limit for the level of ATPase contamination in our preparation of Rad50 (less than 0.025%).

Steady-state Exonuclease Activity of the MR Complex—To continuously monitor the exonuclease activity of the MR complex, we employed the fluorescent nucleotide analog, 2-AP, which has low fluorescence when incorporated into DNA and high fluorescence as a free nucleotide. We performed the assay under steady-state conditions ([DNA] > [enzyme]) with the 2-AP probe located at either the 1 or 17 position relative to the 3′ end of a 50-bp DNA substrate. As seen in Fig. 3*A*, when the 2-AP probe is located at the 1 position, the steady-state exonuclease activity of both the wild-

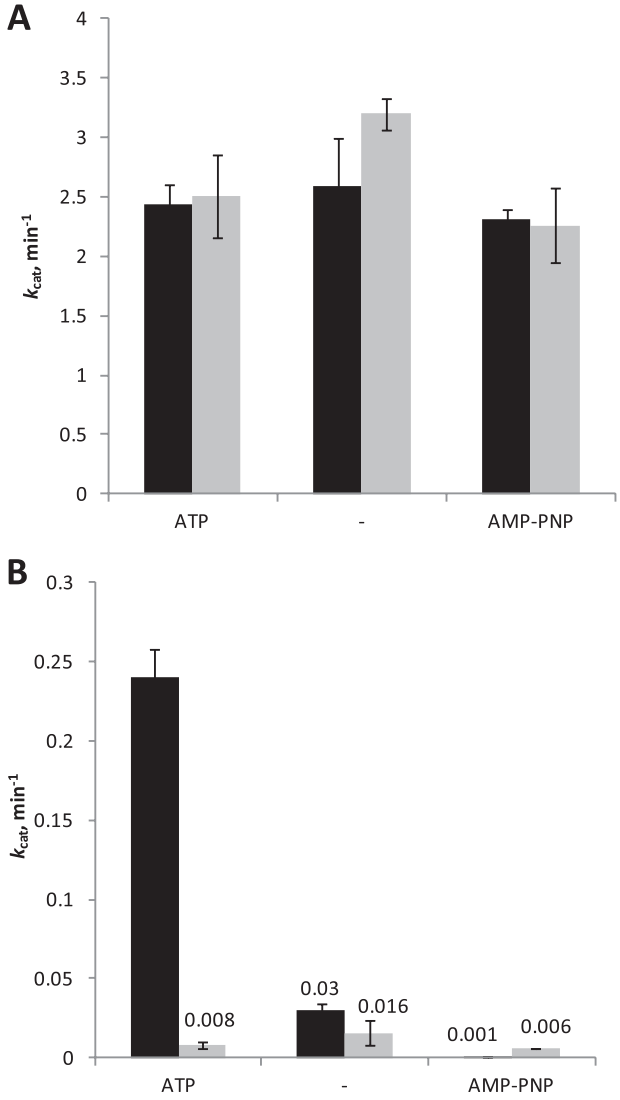

FIGURE 3. **Steady-state exonuclease activity of wild-type and mutant MR complexes.** *A*, exonuclease activity using the 50-bp dsDNA substrate with the 2-AP probe located at the 3′ end of the DNA is shown. The concentrations of DNA, Mre11, Rad50 (wild-type and K42M), ATP, and AMP-PNP were 1.3 μM, 0.105 μM, 0.1 μM, 0.25 mM, and 0.25 mM, respectively. The *black* and *gray bars* represent the wild-type and K42M-Rad50 MR complexes, respectively. *B*, exonuclease activity using the 50-bp dsDNA substrate with the 2-AP probe located at position 17 relative to the 3′ end of the DNA is shown. The concentrations of DNA, Mre11, Rad50 (wild-type and K42M), ATP, and AMP-PNP were 1.3 μM, 0.42 μM, 0.4 μM, 0.25 mM, and 0.25 mM, respectively. The *black* and *gray bars* represent the wild-type and K42M-Rad50 MR complexes, respectively. The *numbers above the low-activity conditions* represent k_{cat} (min^{-1}). The *error bars* for both *A* and *B* represent the S.D. of at least three assays.

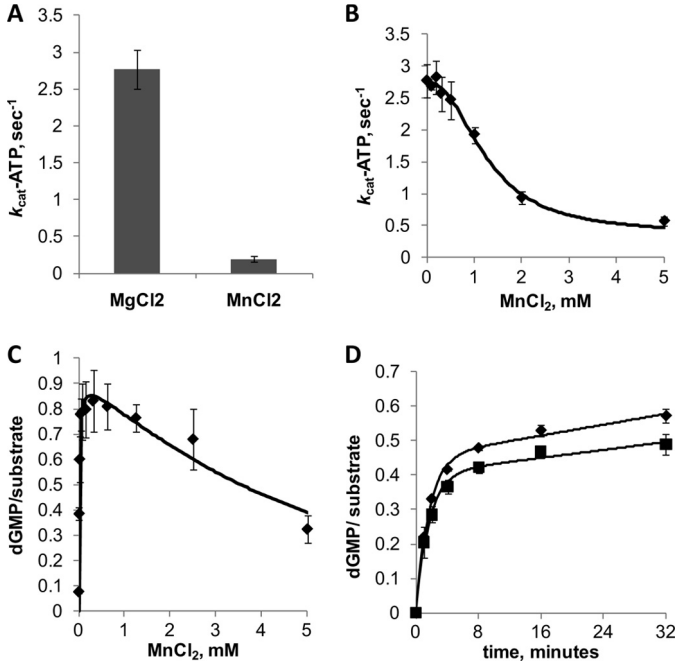

FIGURE 4. **The dependence of Mg^{2+}/Mn^{2+} cation on ATP hydrolysis and dsDNA exonuclease activity.** *A*, the rates of ATP hydrolysis in the presence of 5 mM $MgCl_2$ or $MnCl_2$ are shown. The rates were determined using the coupled fluorometric assay as described under "Experimental Procedures" using Rad50, Mre11, and DNA concentrations of 50, 67, and 260 nM, respectively. *B*, the effect of increasing $MnCl_2$ concentration on the rate of ATP hydrolysis in the presence of 5 mM $MgCl_2$ is shown. The concentrations of Rad50, Mre11, and dsDNA are identical to *panel A*. *C*, quantification of a PEI-TLC exonuclease assay using the uniformly labeled 1.68-kb dsDNA using a fixed concentration of $MgCl_2$ (5 mM) and increasing concentrations of $MnCl_2$ is shown. The concentrations of Rad50, Mre11, and ATP were 0.5 μM, 0.5 μM, and 2 mM, respectively. Each reaction was carried out for 10 min using a dsDNA concentration of 0.024 μM. *D*, shown is the time course of exonuclease activity at 5 mM $MnCl_2$ (*filled diamonds*) or 0.3 mM $MnCl_2$ and 5 mM $MgCl_2$ (*filled squares*) using the uniformly labeled 1.68 kb dsDNA (6 nM) and identical protein and ATP concentrations as *panel C*.

type and K42M-Rad50 MR complex is essentially unaffected by the presence of either ATP or the non-hydrolyzable ATP analog, AMP-PNP (k_{cat} values ranging between 2.3 and 3.2 min^{-1}). When the 2-AP probe is located at the 17 position (Fig. 3*B*), the steady-state exonuclease rate of both wild-type and the K42M-Rad50 MR complex is much reduced compared with the 1 position substrate with k_{cat} values of 0.03 and 0.015 min^{-1}, respectively. The addition of ATP to the wild-type MR complex increases the exonuclease rate (0.24 min^{-1}) but decreases the rate of the K41M-Rad50 MR complex (0.008 min^{-1}). The addition of AMP-PNP decreases the rate of both the wild-type and K42M-Rad50 MR complex with k_{cat} values of 0.001 and 0.006 min^{-1}, respectively.

Metal Dependence of ATP Hydrolysis and Exonuclease Activities—Even though the nuclease activity strongly prefers $MnCl_2$ over $MgCl_2$, the ATP hydrolysis activity of the MR-DNA complex prefers $MgCl_2$ (Fig. 4*A*). Under steady-state conditions, the apparent k_{cat} for ATP hydrolysis in the presence of 5 mM $MgCl_2$ or 5 mM $MnCl_2$ is 2.8 ± 0.3 and 0.23 ± 0.03 s^{-1}, respectively. Because the nuclease activity requires $MnCl_2$, yet under physiological conditions the concentrations of Mg^{2+} far exceeds that of Mn^{2+} (51), we measured the rate of ATP hydrolysis at fixed $MgCl_2$ (5 mM) while varying the concentration of $MnCl_2$ from 0.1 to 5 mM (Fig. 4*B*). The ATP hydrolysis rate is inhibited by $MnCl_2$ with an IC_{50} of 1.3 ± 0.1 mM. We next explored the metal dependence of the nuclease reaction in more detail. We employed the uniformly [α-^{32}P]dGTP-labeled 1.6-kb PCR product as the exonuclease substrate and again varied the concentration of $MnCl_2$ in the presence of 5 mM $MgCl_2$ (Fig. 4*C*). The nuclease activity sharply increased between $MnCl_2$ concentrations of 0 and 0.1 mM followed by a slow decrease in nuclease activity between 0.4 and 5 mM. This data can be fit using the following uncompetitive substrate inhibition equation,

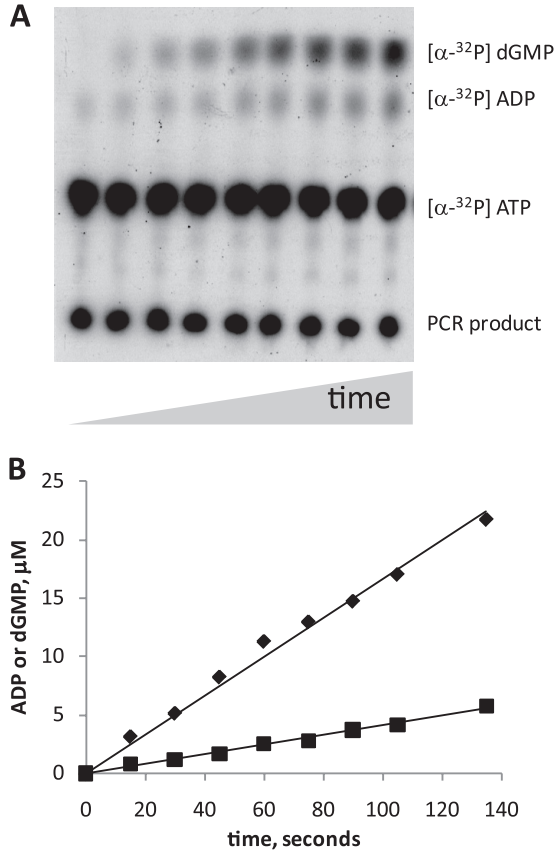

FIGURE 5. **Kinetics of the Mre11-Rad50 dsDNA exonuclease reaction.** *A*, an exonuclease reaction time course analyzed via PEI-TLC is shown. The substrates (DNA and ATP) and products (ADP and dGMP) can be simultaneously monitored. The reactions were performed at 37 °C containing Rad50 (0.5 μM), Mre11 (0.5 μM), ATP (2 mM), $MgCl_2$ (5 mM), $MnCl_2$ (0.3 mM), and 1.68 kb DNA (0.024 μM). *B*, shown is quantification of the PEI-TLC plate shown in *A*. The *filled diamonds* represent the exonuclease reaction product (dGMP), and the *filled squares* represent the ATP hydrolysis product (ADP).

$$v = \frac{V_{max} \cdot [A]}{K_a + [A]\left(1 + \frac{[A]}{K_i}\right)} \qquad \text{(Eq. 2)}$$

where v is velocity, V_{max} is the maximal velocity at saturating activator concentration, K_a is the Michaelis constant for the activator (concentration of A where $v = 0.5 \cdot V_{max}$), and K_i is the inhibition constant. The data-fitting yielded a K_a Mn^{2+} of 0.011 ± 0.002 mM and K_i Mn^{2+} of 4.1 ± 0.8 mM. Finally, we compared the MR complex nuclease activity with 5 mM $MnCl_2$ alone or with 5 mM $MgCl_2$ and 0.3 mM $MnCl_2$ in combination (Fig. 4*D*). The results of this assay indicate that the nuclease activity is essentially identical under both of these conditions.

Rad50 ATP Hydrolysis and Utilization during the Exonuclease Reaction—A TLC-based assay was employed to simultaneously monitor the ATP hydrolysis and exonuclease activity of Rad50 and Mre11, respectively, using $MgCl_2$ and $MnCl_2$ concentrations of 5 and 0.3 mM, respectively (Fig. 5*A*). To visualize both DNA and ATP, we used a uniformly [α-^{32}P]dGTP-labeled 1.6-kb PCR product as the DNA substrate and ATP that was labeled at the α-phosphate with ^{32}P. The concentration of ATP was held at 0.2 mM, which is ~4-fold above the K_m ATP for the MR complex (Table 1). The TLC assay enables visualization of both ATP/ADP and DNA/dGMP, making the determination of ATP utilization highly accurate. The MR complex was held in excess over the DNA substrate so that the rate of exonuclease activity reflects the rate of nucleotide excision and translocation and not productive DNA binding. As seen in Fig. 5*B*, the rate of exonuclease and ATPase activity is 0.1664 and 0.0408 $\mu M/s^{-1}$, respectively. This suggests that approximately four bases are removed for every ATP hydrolyzed. The concentration of dsDNA ends in this assay is 0.0217 μM, which represents the upper limit for the concentration of DNA-bound MR complex. Assuming a fully saturated dsDNA substrate during the exonuclease reaction, the k_{cat} for ATP hydrolysis is then 1.9 s^{-1} and the maximum rate of nucleotide removal is 7.67 s^{-1}.

TABLE 2
The effect of UvsY and gp32 (T4 SSB) on ATPase activity of the Mre11/Rad50

Protein complex[a]	k_{cat}[b]
	s^{-1}
Mre11/Rad50/DNA	3.2 ± 0.1
Mre11/Rad50/DNA/UvsY	2.5 ± 0.4
Mre11/Rad50/DNA/gp32	2.9 ± 0.2
Mre11/Rad50/DNA/UvsY/gp32	1.7 ± 0.1

[a] Concentrations were: Mre11, 83 nM; Rad50, 67 nM; DNA, 1 μM; UvsY, 550 nM; gp32, 524 nM.
[b] Results are the apparent k_{cat} (rate measured at saturating concentrations of ATP and DNA). The values reported are the average of three individual measurements. Errors represent the S.D.

The Effect of T4 UvsY and gp32 Proteins on the Exonuclease Activity of the MR Complex—Consistent with MR complexes from human, *P. furiosus*, and *S. cerevisiae*, Mn^{2+} is the preferred metal for the exonuclease reaction in the T4 system. However, because physiological concentrations of Mg^{2+} far exceed those of Mn^{2+} (51), we further explored the ability of Mg^{2+} to support exonuclease activity. To quantify the exonuclease activity of the MR complex with Mg^{2+} and Mn^{2+}, we employed the uniformly [α-^{32}P] dGTP-labeled 1.6-kb PCR product and the TLC assay (Fig. 6). Protein was held in excess over the dsDNA substrate; therefore, the loss of product can be fitted to a single-exponential decay with rate constants of 0.105 ± 0.001 and 0.009 ± 0.0005 min^{-1} for Mn^{2+} and Mg^{2+}, respectively (an 11-fold difference between Mn^{2+} and Mg^{2+}). We then tested the effect of UvsY and gp32 on the exonuclease rates in the presence of either Mg^{2+} or Mn^{2+}. UvsY and gp32 were chosen as possible candidates for the modulation of MR complex activity because these two proteins bind to the product of the MR reaction (*i.e.* ssDNA) and participate in the subsequent step of DSB repair (strand invasion). We found that the presence of UvsY and gp32 increased the Mg^{2+}-dependent reaction by nearly 5-fold (rate constant of 0.0410 ± 0.0037 min^{-1}) while having no effect on the rate of the Mn^{2+}-dependent reaction (rate constant of 0.1031 ± 0.0104 min^{-1}). Separately, UvsY and gp32 had no measurable effect on the Mg^{2+}-dependent nuclease activity (data not shown). Several control experiments were performed to rule out the possibility of nuclease contamination in our preparations of UvsY and gp32 (Fig. 6). The Mg^{2+}-dependent exonuclease reaction required Rad50, Mre11, UvsY, gp32, and ATP. Omission of Rad50, Mre11, or ATP resulted in a complete

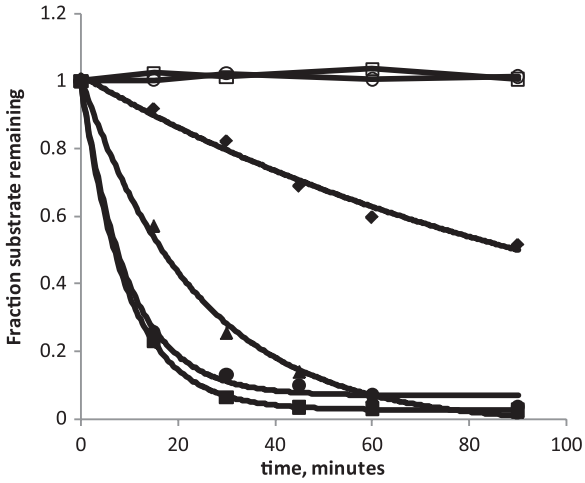

FIGURE 6. **The effect of UvsY and gp32 on the $MgCl_{2+}$-dependent exonuclease reaction.** Shown is quantification of a PEI-TLC exonuclease assay using the uniformly labeled 1.68-kb dsDNA. Reactions contained Rad50 (0.5 μM), Mre11 (0.5 μM), UvsY (1 μM, hexamer), gp32 (1 μM), ATP (2 mM), and either MgC_{l2} or $MnCl_2$ (5 mM). The conditions are: $MnCl_2$, Mre11, Rad50, and ATP (*filled squares*); $MgCl_2$, Mre11, Rad50, and ATP (*filled diamonds*); $MnCl_2$, Mre11, Rad50, UvsY, gp32, and ATP (*filled circles*); $MgCl_2$, Mre11, Rad50, UvsY, gp32, and ATP (*filled triangles*); $MgCl_2$, UvsY, gp32, and ATP (*open squares*); $MgCl_2$, Mre11, Rad50, UvsY, gp32, and ATP omission (*open circles*).

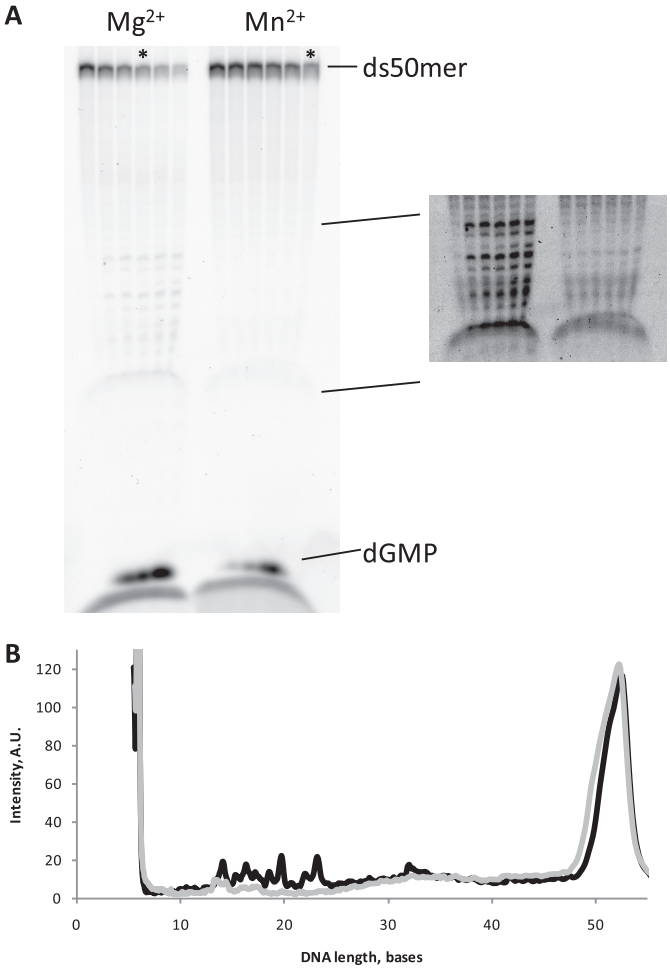

FIGURE 7. **Comparison of nuclease products in reactions containing UvsY and gp32 with $MgCl_{2+}$ and $MnCl_{2+}$.** *A*, analysis of nuclease reaction products using 16% UREA-PAGE is shown. The time points for both reactions are 0, 0.5, 1, 2, 4, and 8 min. The concentrations of the Mre11, Rad50, and ATP for the $MgCl_2$ (5 mM)-containing reaction were 0.1 μM, 0.1 μM. and 2 mM, respectively. The concentrations of the Mre11, Rad50, and ATP for the $MnCl_2$ (5 mM)-containing reaction were 0.025 μM, 0.025 μM, and 2 mM, respectively. The concentrations of UvsY, gp32, and the 5′-^{32}P-labeled 50-bp dsDNA for both reactions were 1, 1, and 0.5 μM, respectively. The *inset* highlights the portion of the gel corresponding to mobility between 25 and 15 bases. *B*, shown is size distribution of the products contained in *lane 4* of the Mg^{2+}-dependent reaction (*black*) and *lane 6* of the Mn^{2+}-dependent reaction (*light gray*). These *lanes* are indicated by *asterisks* at the *top of the gel*. The nearly overlapping traces at the 50 base positions indicate that the reaction has proceeded to the same extent. *A.U.*, arbitrary units.

loss of the exonuclease activity, strongly arguing against the introduction of a contaminating nuclease present in the preparations of UvsY or gp32. We also examined the effect of UvsY and gp32 on the steady-state rate of ATP hydrolysis by the MR complex in the presence of a DNA substrate (Table 2). Separately, UvsY and gp32 did not significantly alter the rate, whereas the combination reduced the rate by 1.9-fold.

The polarity of the UvsY/gp32-enhanced, Mg^{2+}-dependent exonuclease reaction was examined under steady-state conditions using 3′-labeled 50-bp dsDNA. This substrate was chosen because the appearance of any DNA products of intermediate size represents a deviation from the strict 3′ to 5′ exonuclease reaction that was observed in Fig. 2. Under steady-state conditions (which are required when short DNA substrates are used), the Mg^{2+}-dependent reaction in the absence of UvsY/gp32 is nearly undetectable (*i.e.* the UvsY/gp32 enhancement of the steady-state Mg^{2+}-dependent reaction appears greater than the 5-fold observed in Fig. 6). Therefore, we compared the Mn^{2+}-dependent reaction to the Mg^{2+}-dependent reaction, both, in the presence of UvsY/gp32. As shown in Fig. 7, in contrast to the reaction in the presence of Mn^{2+}, the Mg^{2+}-dependent reaction results in products with a length ranging between 15 and 25 bases, suggesting that an additional form of nuclease activity has occurred. Quantitation of this reaction reveals that ~32% of the products were between 15 and 25 bases with the remaining 68% as dGMP.

DISCUSSION

Bacteriophage T4 is a well established model system for investigating the biochemistry of proteins involved in DNA replication, recombination, and repair (3, 52, 53). Studies using the T4 phage model system led to the first proposed model for recombination-dependent DNA replication (RDR) (54). The RDR model begins with the formation of a single-stranded 3′ DNA end that subsequently undergoes strand invasion and pairing with a homologous dsDNA template. The single-stranded 3′ DNA can be formed as a result of incomplete replication of the lagging strand or through the action of a nuclease. Over the past three decades since the RDR model was proposed, all of the enzymes and proteins that are required to carry out RDR in T4 have been isolated and extensively characterized biochemically, with the notable exception of the nuclease complex thought to be responsible for the creation of the 3′ ssDNA overhangs (Rad50 (gp46) and Mre11 (gp47)). Here we have described for the first time the expression, purification, and biochemical characterization of the Rad50 and Mre11 proteins from bacteriophage T4.

On a qualitative level it appears that the various activities of the MR complex are well conserved between all three kingdoms of life. The T4 MR complex is an ATPase, an ssDNA

endonuclease, and a 3′ to 5′ dsDNA exonuclease. ATP hydrolysis is positively cooperative and is activated by the presence of Mre11 and DNA. We have found that during repetitive dsDNA exonuclease activity, ~4 nucleotides are removed for every ATP that is hydrolyzed, and the maximum exonuclease rate is 7.7 nucleotides/s. ATP hydrolysis increases the rate of multiple nucleotide excisions but does not alter the rate of the first nucleotide excision. Interestingly, we have found that two T4 phage proteins that are necessary for the subsequent steps of RDR/DSB repair activate the Mg^{2+}-dependent nuclease reaction, which produces an altered product profile as compared with the Mn^{2+}-dependent exonuclease reaction.

To our knowledge, this is the first instance that the steady-state ATP hydrolysis rate constants have been reported for a Rad50 homolog in the presence and absence of Mre11 and a DNA substrate. We found that by itself, Rad50 is a relatively inefficient ATPase, with a k_{cat} of 0.15 s^{-1}. The reaction is mildly positively cooperative with a Hill coefficient of 1.4, indicating Rad50 is a least a dimer, consistent with the structural analysis of *Pfu* Rad50 and other ABC proteins (31, 32). Separately, the addition of DNA or Mre11 to Rad50 resulted in very minor perturbations in the kinetic parameters of Rad50. In contrast, the addition of both Mre11 and DNA resulted in a 20-fold increase in k_{cat} and an increase in the Hill coefficient to 2.4. These reactions are performed with Mg^{2+} as the only divalent cation so that there is essentially no nuclease activity under these conditions. This indicates that ATP hydrolysis can be uncoupled from nuclease activity and suggests that Mre11 and dsDNA act as allosteric activators of Rad50. The increase in the Hill coefficient from 1.4 to 2.4 suggests that in the presence of Mre11 and dsDNA, there are more than two ATP sites in communication with each other. It is not clear how this might occur, but it is tempting to speculate that binding of dsDNA promotes hetero-octamer $(Mre11_2/Rad50_2)_2$ formation through zinc-hook-mediated tethering of the Rad50 coiled-coil domains (15). Hetero-octamers of the *Pfu* MR complex have been previously observed in electron microscopy (33), and atomic force microscopy experiments (55) have revealed that DNA binding results in a straightening of Rad50 coiled-coils, which prevents an intracomplex tether (hetero-tetramer) and promotes an intercomplex tether (hetero-octamer).

The exact function of Rad50 ATP hydrolysis activity has been unclear (56). Based on structural changes between the ATP-free and bound forms of *Pfu* Rad50, it has been proposed that ATP hydrolysis induces a conformational change that may promote product release (dNMP) or drive MR complex translocation (31). Our data are inconsistent with the product release model, as the rate of excision of the first nucleotide at the 3′ end of the DNA is not affected by ATP. Additionally, the stoichiometry of ATP hydrolysis is one ATP per four nucleotides removed. If ATP hydrolysis was directly linked to product release, then a 1:1 correspondence between ATP hydrolysis and nucleotide removal would be expected. The data are more consistent with ATP being involved in the translocation of the MR complex after nucleotide excision and release. Because ATP and AMP-PNP do not affect the rate of the first nucleotide excision for either the wild-type or K42M-Rad50 MR complexes, it is unlikely that the MR complex must unwind or open the DNA duplex before nucleotide excision. In contrast, ATP hydrolysis increased the exonuclease rate when the probe is moved 17 bases away from the 3′ end, indicating that ATP hydrolysis is necessary for multiple, processive nucleotide excisions. This suggests that the energy of ATP hydrolysis likely drives translocation of the MR complex. Consistent with this, when the probe is in the 17 position, AMP-PNP potently inhibits the exonuclease activity of the wild-type enzyme, and both ATP and AMP-PNP inhibit the K42M-Rad50 MR complex. The observed inhibition is likely due to the stalling of the MR complex after nucleotide excision and product release (*i.e.* the MR complex is unable to translocate or dissociate from the DNA in the ATP-bound form). In the absence of ATP, the MR complex likely dissociates from the DNA substrate and rebinds at the new ss/dsDNA junction (non-processively). If this interpretation is correct, then the steady-state exonuclease rate constant in the presence of AMP-PNP is equal to the rate of dissociation of the MR complex from DNA. The 1:4 ATP/base stoichiometry suggests that the Mre11 is able to remove four nucleotides before it is required to translocate to the new ss/dsDNA junction. This would require "scrunching" of the DNA, similar to that which has been proposed for the NS3 helicase (57).

The data shown in Fig. 2 are consistent with a 3′ to 5′ dsDNA exonuclease. This activity is at odds with the proposed physiological function of the MR complex, a paradox that has been long recognized (15, 58, 59). It is conceivable that the observed 3′ to 5′ exonuclease activity is the relevant physiological activity and the MR complex does not directly participate in the production of a 3′ ssDNA overhangs. However, this possibility seems unlikely for the following reasons; 1) it is well established that in eukaryotes the nuclease activity of the MR complex is required for the removal of Spo11/Rec12, which is covalently linked to the 5′ end of the DSB during meiosis (60), 2) the nuclease activity of Mre11 is required for the removal of topoisomerase-5′ DNA covalent adducts that are stabilized by anti-cancer etoposide derivatives (10), 3) the nuclease activity of Mre11 is required for repair of ionizing radiation-induced DSBs (38), and 4) in T4 phage, Mre11 and Rad50 are necessary for the initiation of recombination-dependent replication and recombination-dependent DSB repair, which begins with the 5′ to 3′ resection of a DNA end (7, 61). Even with the above data, the precise role of the MR complex in DSB repair is still an open question, and the polarity paradox remains. Therefore, we tested several T4 recombination proteins for a possible change in the nuclease mechanism of the T4 MR complex. In the presence of $MnCl_2$, we did not observe any significant differences in the rate or product profile of MR nuclease assays in the presence of UvsX, gp32, and UvsY either alone or in combination. However, UvsY and gp32 were found to enhance the ability of the T4 MR complex to utilize $MgCl_2$ as a cofactor for the nuclease activity. We examined the product profile of the $MgCl_2$-dependent reaction in the presence of UvsY and gp32, and in addition to the dGMP that is produced by 3′ to 5′ exonuclease activity, we also observed a distribution of

products in the size range of 15–25 bases. These products could be the result of a 5′ to 3′ exonuclease or an endonuclease activity. We favor an endonuclease mechanism due to the absence of products between 50 and 25 bases, which would be produced if 5′ to 3′ exonuclease activity had occurred. Experiments are currently under way to determine the exact nature of the alteration in nuclease mechanism. A metal-dependent change nuclease mechanism has also been observed in the MR complex from the thermophilic organism *P. furiosus* when assayed at elevated (physiologically relevant) temperatures (59). In the case of the *Pfu* MR complex, the $MgCl_2$-dependent reaction produces a 3′ ssDNA overhang through endonucleolytic cleavage of sites close to the 5′ end of the dsDNA, similar to what we are proposing here for the T4 MR complex.

The mechanism behind the increased ability to use Mg^{2+} as a cofactor is not clear but likely involves physical interaction(s) between the MR complex and UvsY/gp32. Based on our observation that 5 mM $MgCl_2$ does not inhibit the nuclease activity of the complex even when the concentration of $MnCl_2$ is 50-fold lower (0.1 mM), it appears that the affinity of Mg^{2+} for the Mre11 active site is low compared with Mn^{2+}. This is consistent with the fact that Mre11 crystals grown in the presence of $MgCl_2$ only have one of the two required divalent cation sites occupied (62). If this is correct and Mre11 normally has weak affinity for $MgCl_2$, then it is plausible to assume that UvsY and gp32 act in an allosteric manner to increase the affinity of Mg^{2+} for the active site of Mre11. This hypothesis requires that gp32 and/or UvsY directly interact with the MR complex, which has been previously observed in T4 phage lysate (63). Additionally, *in vivo* experiments have strongly suggested a physical interaction between gp32 and the MR complex (64). To enhance the affinity of Mg^{2+} for Mre11, the interaction of gp32 and/or UvsY with the MR complex would have to reorient the active site in some manner. The nature of this putative active site perturbation is unclear and may require crystallographic analysis of the T4 MR complex.

The mechanism behind the Mg^{2+}-dependent change in product profile is also not clear and will require further investigation. One hypothesis is that the ssDNA endonuclease activity of the MR complex is enhanced in the presence of Mg^{2+} and UvsY/gp32. This requires at least transient melting of the DNA duplex, which is an activity that has been previously observed in gp32 (65, 66). If gp32 and/or UvsY were also to protect the 3′ but not the 5′ strand of the DNA from endonucleolytic cleavage, then this would result in the production of a 3′ ssDNA overhang that is pre-bound with UvsY and gp32 and primed for the next step of recombination, filament formation by UvsX. It is clear from the data shown in Fig. 7 that even in the presence of UvsY and gp32, there is still a high level of 3′ to 5′ dsDNA exonuclease activity (nearly 70% of the products are produced as a result of exonuclease activity). This may indicate that additional proteins are required for the efficient production of a 3′ ssDNA overhang. Based on recent results from *S. cerevisiae* and *P. furiosus*, which demonstrated the involvement of helicases in MR-dependent DSB resection (42, 59), a possible candidate is UvsW helicase. UvsW helicase is known to be necessary for DSB repair (67, 68) and is a functional analog of Sgs1, which is the *S. cerevisiae* helicase involved in DSB resection. We are currently in the process of testing the above hypothesis.

With the biochemical characterization of the bacteriophage T4 MR complex reported here, the entire complement of T4 phage proteins involved in recombination and DSB repair have been purified and assayed *in vitro*. The bacteriophage T4 system provides milligram quantities of purified Mre11 and Rad50, which is not currently possible in the eukaryotic systems. Given the apparent conservation in DNA repair mechanisms between all kingdoms of life, it is expected that the T4 phage model system will provide valuable mechanistic insights into what has been termed the "keystone complex" of DNA repair (69).

Acknowledgments—S. W. Nelson thanks Stephen J. Benkovic for allowing him to initiate this project while he was a postdoctoral fellow at Pennsylvania State University and to continue the project at Iowa State University.

REFERENCES

1. Mosig, G., Colowick, N., Gruidl, M. E., Chang, A., and Harvey, A. J. (1995) *FEMS Microbiol. Rev.* **17,** 83–98
2. Belanger, K. G., and Kreuzer, K. N. (1998) *Mol. Cell* **2,** 693–701
3. Mosig, G. (1998) *Annu. Rev. Genet.* **32,** 379–413
4. Miller, E. S., Kutter, E., Mosig, G., Arisaka, F., Kunisawa, T., and Rüger, W. (2003) *Microbiol. Mol. Biol. Rev* **67,** 86–156
5. George, J. W., Stohr, B. A., Tomso, D. J., and Kreuzer, K. N. (2001) *Proc. Natl. Acad. Sci. U.S.A.* **98,** 8290–8297
6. Lielausis, A., Epstein, R. H., Bolle, A., Steinberg, C. M., Kellenberger, E., Boy De La Tour, E., Chevalley, R., Edgar, R. S., Susman, M., and Denhardt, G. H. (1963) *Cold Spring Harbor Symposia on Quantitative Biology*, p. 375
7. George, J. W., and Kreuzer, K. N. (1996) *Genetics* **143,** 1507–1520
8. Krogh, B. O., and Symington, L. S. (2004) *Annu. Rev. Genet* **38,** 233–271
9. Helleday, T., Lo, J., van Gent, D. C., and Engelward, B. P. (2007) *DNA Repair* **6,** 923–935
10. Povirk, L. F. (2006) *DNA Repair* **5,** 1199–1212
11. Shrivastav, M., De Haro, L. P., and Nickoloff, J. A. (2008) *Cell Res.* **18,** 134–147
12. San Filippo, J., Sung, P., and Klein, H. (2008) *Annu. Rev. Biochem.* **77,** 229–257
13. Valerie, K., and Povirk, L. F. (2003) *Oncogene* **22,** 5792–5812
14. Dillingham, M. S., and Kowalczykowski, S. C. (2008) *Microbiol. Mol. Biol. Rev* **72,** 642–671
15. Connelly, J. C., and Leach, D. R. F. (2002) *Trends Biochem. Sci.* **27,** 410–418
16. Roca, A. I., and Cox, M. M. (1997) *Prog. Nucleic Acid Res. Mol. Biol* **56,** 129–223
17. Kreuzer, K. N. (2005) *Annu. Rev. Microbiol.* **59,** 43–67
18. Symington, L. S. (2002) *Microbiol. Mol. Biol. Rev* **66,** 630–670
19. Raaijmakers, H., Vix, O., Törö, I., Golz, S., Kemper, B., and Suck, D. (1999) *EMBO J.* **18,** 1447–1458
20. Hinton, D. M., and Nossal, N. G. (1986) *J. Biol. Chem.* **261,** 5663–5673
21. Derr, L. K., and Kreuzer, K. N. (1990) *J. Mol. Biol.* **214,** 643–656
22. Morrical, S. W., and Alberts, B. M. (1990) *J. Biol. Chem.* **265,** 15096–150103
23. Shamoo, Y., Friedman, A. M., Parsons, M. R., Konigsberg, W. H., and Steitz, T. A. (1995) *Nature* **376,** 362–366
24. Nelson, S. W., Zhuang, Z., Spiering, M. M., and Benkovic, S. J. (2009) *Viral Genome Replication*, pp. 337–364, Springer, New York
25. Sharples, G. J., and Leach, D. R. (1995) *Mol. Microbiol.* **17,** 1215–1217

26. Ivanov, E. L., Sugawara, N., White, C. I., Fabre, F., and Haber, J. E. (1994) *Mol. Cell Biol.* **14,** 3414–3425
27. Trujillo, K. M., Yuan, S. S., Lee, E. Y., and Sung, P. (1998) *J. Biol. Chem.* **273,** 21447–21450
28. Trujillo, K. M., and Sung, P. (2001) *J. Biol. Chem.* **276,** 35458–35464
29. Oldham, M. L., Davidson, A. L., and Chen, J. (2008) *Curr. Opin. Struct. Biol.* **18,** 726–733
30. Davidson, A. L., Dassa, E., Orelle, C., and Chen, J. (2008) *Microbiol. Mol. Biol. Rev.* **72,** 317–364
31. Hopfner, K. P., Karcher, A., Shin, D. S., Craig, L., Arthur, L. M., Carney, J. P., and Tainer, J. A. (2000) *Cell* **101,** 789–800
32. Hopfner, K. P., and Tainer, J. A. (2003) *Curr. Opin. Struct. Biol.* **13,** 249–255
33. Hopfner, K., Craig, L., Moncalian, G., Zinkel, R. A., Usui, T., Owen, B. A. L., Karcher, A., Henderson, B., Bodmer, J., McMurray, C. T., Carney, J. P., Petrini, J. H. J., and Tainer, J. A. (2002) *Nature* **418,** 562–566
34. Lee, J. H., and Paull, T. T. (2006) *Methods Enzymol.* **408,** 529–539
35. Hopfner, K. P., Karcher, A., Shin, D., Fairley, C., Tainer, J. A., and Carney, J. P. (2000) *J. Bacteriol.* **182,** 6036–6041
36. Barford, D., Das, A. K., and Egloff, M. P. (1998) *Annu. Rev. Biophys. Biomol. Struct.* **27,** 133–164
37. Bressan, D. A., Baxter, B. K., and Petrini, J. H. (1999) *Mol. Cell Biol.* **19,** 7681–7687
38. Buis, J., Wu, Y., Deng, Y., Leddon, J., Westfield, G., Eckersdorff, M., Sekiguchi, J. M., Chang, S., and Ferguson, D. O. (2008) *Cell* **135,** 85–96
39. Stewart, G. S., Maser, R. S., Stankovic, T., Bressan, D. A., Kaplan, M. I., Jaspers, N. G., Raams, A., Byrd, P. J., Petrini, J. H., and Taylor, A. M. (1999) *Cell* **99,** 577–587
40. Williams, R. S., Moncalian, G., Williams, J. S., Yamada, Y., Limbo, O., Shin, D. S., Groocock, L. M., Cahill, D., Hitomi, C., Guenther, G., Moiani, D., Carney, J. P., Russell, P., and Tainer, J. A. (2008) *Cell* **135,** 97–109
41. Mimitou, E. P., and Symington, L. S. (2008) *Nature* **455,** 770–774
42. Zhu, Z., Chung, W. H., Shim, E. Y., Lee, S. E., and Ira, G. (2008) *Cell* **134,** 981–994
43. Sambrook, J. F., Maniatis, T., and Sambrook, J. F. (1989) *Molecular Cloning: A Laboratory Manual*, pp. 3.30–3.32, Cold Spring Harbor Laboratory Press, Cold Spring Harbor, NY
44. Valentine, A. M., Ishmael, F. T., Shier, V. K., and Benkovic, S. J. (2001) *Biochemistry* **40,** 15074–15085
45. Bloom, L. B., Otto, M. R., Eritja, R., Reha-Krantz, L. J., Goodman, M. F., and Beechem, J. M. (1994) *Biochemistry* **33,** 7576–7586
46. Gilbert, S. P., and Mackey, A. T. (2000) *Methods* **22,** 337–354
47. Paull, T. T., and Gellert, M. (1998) *Mol. Cell* **1,** 969–979
48. Chong, S., Mersha, F. B., Comb, D. G., Scott, M. E., Landry, D., Vence, L. M., Perler, F. B., Benner, J., Kucera, R. B., Hirvonen, C. A., Pelletier, J. J., Paulus, H., and Xu, M. Q. (1997) *Gene* **192,** 271–281
49. Bleuit, J. S., Xu, H., Ma, Y., Wang, T., Liu, J., and Morrical, S. W. (2001) *Proc. Natl. Acad. Sci. U.S.A.* **98,** 8298–8305
50. Bhaskara, V., Dupré, A., Lengsfeld, B., Hopkins, B. B., Chan, A., Lee, J. H., Zhang, X., Gautier, J., Zakian, V., and Paull, T. T. (2007) *Mol. Cell* **25,** 647–661
51. Berg, J. M., and Lippard, S. (1994) *Principles of Bioinorganic Chemistry*, pp. 103–111, University Science Books, Mill Valley, CA
52. Nossal, N. G. (1992) *FASEB J.* **6,** 871–878
53. Benkovic, S. J., Valentine, A. M., and Salinas, F. (2001) *Annu. Rev. Biochem.* **70,** 181–208
54. Mosig, G., Ehring, R., and Duerr, E. O. (1968) *Cold Spring Harb. Symp. Quant. Biol.* **33,** 361–369
55. Moreno-Herrero, F., de Jager, M., Dekker, N. H., Kanaar, R., Wyman, C., and Dekker, C. (2005) *Nature* **437,** 440–443
56. Kinoshita, E., van der Linden, E., Sanchez, H., and Wyman, C. (2009) *Chromosome Res.* **17,** 277–288
57. Myong, S., Bruno, M. M., Pyle, A. M., and Ha, T. (2007) *Science* **317,** 513–516
58. Assenmacher, N., and Hopfner, K. P. (2004) *Chromosoma* **113,** 157–166
59. Hopkins, B. B., and Paull, T. T. (2008) *Cell* **135,** 250–260
60. Borde, V. (2007) *Chromosome Res.* **15,** 551–563
61. Stohr, B. A., and Kreuzer, K. N. (2002) *Genetics* **162,** 1019–1030
62. Hopfner, K. P., Karcher, A., Craig, L., Woo, T. T., Carney, J. P., and Tainer, J. A. (2001) *Cell* **105,** 473–485
63. Formosa, T., Burke, R. L., and Alberts, B. M. (1983) *Proc. Natl. Acad. Sci. U.S.A.* **80,** 2442–2446
64. Mosig, G., and Bock, S. (1976) *J. Virol.* **17,** 756–761
65. Hosoda, J., Takacs, B., and Brack, C. (1974) *FEBS Lett.* **47,** 338–342
66. Pant, K., Karpel, R. L., and Williams, M. C. (2003) *J. Mol. Biol.* **327,** 571–578
67. Carles-Kinch, K., George, J. W., and Kreuzer, K. N. (1997) *EMBO J.* **16,** 4142–4151
68. Nelson, S. W., and Benkovic, S. J. (2007) *J. Biol. Chem.* **282,** 407–416
69. Williams, R. S., Williams, J. S., and Tainer, J. A. (2007) *Biochem. Cell Biol.* **85,** 509–520

Biochemical Characterization of Bacteriophage T4 Mre11-Rad50 Complex

Timothy J. Herdendorf, Dustin W. Albrecht, Stephen J. Benkovic and Scott W. Nelson

J. Biol. Chem. 2011, 286:2382-2392.
doi: 10.1074/jbc.M110.178871 originally published online November 15, 2010